Published in International Journal of Engineering Science
Volume 205, 2024, 104158

https://doi.org/10.1016/j.ijengsci.2024.104158

Effects of interfacial sliding on anti-plane waves in an elastic plate imperfectly attached to an elastic half-space

Gennadi I. Mikhasev[a,*], Victor A. Eremeyev[b,c]

[a] *Department of Astronautical Science and Mechanics, Harbin Institute of Technology, P.O. Box 301, 92 West Dazhi Street, 150001 Harbin, China*
[b] *Department of Civil and Environmental Engineering and Architecture (DICAAR), University of Cagliari, Via Marengo, 2, 09123 Cagliari, Italy*
[c] *Gdańsk University of Technology, ul. Gabriela Narutowicza 11/12, 80-233 Gdańsk, Poland*

Abstract

We study the anti-plane shear waves in a domain consisting of an elastic layer (plate) with a coating attached to an elastic half-space (substrate). We assume an imperfect contact between the layer and the half-space, allowing some sliding. We also assume some elastic bonds between the layer and the substrate. On the free top surface we apply the compatibility conditions within the Gurtin-Murdoch surface elasticity. We found two different solutions: (i) the transversely exponential – transversely exponential (TE-TE) regime with amplitudes decaying exponentially from the free top surface and the interface in both the plate and the half-space, and (ii) the transversely harmonic – transversely exponential (TH-TE) regime with harmonic wave behaviour in the transverse direction in the plate and exponential decay in the half-space. The TE regime of anti-plane waves in an elastic half-space with non-perfect contact is also considered as a special case. A detailed analysis of the derived dispersion relations reveals a crucial influence of the interface stiffness on the phase velocities of anti-plane waves. This effect consists in the decrease of the phase velocities when the interfacial bonds are weakened. The strongest effect of the interfacial sliding on the phase veloci-

*Corresponding author.
Email addresses: mikhasev@hit.edu.cn (Gennadi I. Mikhasev), eremeyev.victor@gmail.com (Victor A. Eremeyev)

ties was observed for the long-length waves belonging to the TE-TE regime. Based on the derived lower bounds for the wave numbers from which the TE-TE regime of anti-plane waves exists, we have developed the theoretical background and methodology for assessing the bond stiffness of thin plates imperfectly bonded to an elastic substrate.

Keywords: surface elasticity, imperfect contact, Gurtin-Murdoch model, interfacial sliding, anti-plane waves, dispersion relations, bond stiffness

---

Introduction

The study of surface waves is a rather old but still topical branch of the mechanics and physics of solids and fluids, see for example the classic books by Achenbach (1973); Überall (1973); Ewing et al. (1957); Brekhovskikh (1960); Whitham (1999), the recent review by Kaplunov and Prikazchikov (2017), and the references therein. In particular, these waves could be useful for evaluating near-surface properties of materials. At small scales, various surface-related phenomena, such as surface tension or surface stress, can significantly influence the propagation of surface and interfacial waves. Such an extension of classical linear elasticity to small scales could be based on the surface elasticity approach introduced by Gurtin and Murdoch (1975, 1978) and later generalised by Steigmann and Ogden (1997, 1999), see also Eremeyev (2020); Rodriguez (2024) for further extensions. Such a strain gradient type extension could be necessary for proper description of microstructured coatings Eremeyev et al. (2024). Within this approach one introduces additional constitutive equations at the surface or interface, for example a surface strain density and a surface kinetic energy density. Within the Gurtin-Murdoch surface elasticity there are two length scale parameters, static and dynamic. These give us the ability to capture different size effects observed at small scales. For further discussion of surface elasticity we refer to (Duan et al., 2008; Wang et al., 2011; Javili et al., 2013; Eremeyev, 2016; Mogilevskaya et al., 2021) and the references therein.

Similar to surface tension and capillary waves in fluids Whitham (1999), surface stresses essentially affect the propagation of surface and interfacial waves in solids, see e.g. Gurtin and Murdoch (1978); Murdoch (1976, 1977); Steigmann and Ogden (2007). Moreover, within surface elasticity there is a new class of surface waves called anti-plane surface waves, see Murdoch (1977); Xu and Fan (2015); Eremeyev et al. (2016). It is similar to the clas-

sic Love waves in solids. These waves were studied in a series of papers by Zhu et al. (2019); Eremeyev (2020); Mikhasev et al. (2021, 2022, 2023, 2024), where both perfect and non-perfect interfaces were discussed. Note that the jump conditions for non-perfect interfaces within linear surface elasticity are almost identical to those derived by Mishuris et al. (2006b,a); see also the discussion in Gorbushin et al. (2020) and Mishuris et al. (2012, 2020a,b). In addition, non-perfect contact with sliding can significantly influence the dispersion curves and the nature of wave propagation, see Eremeyev et al. (2016). The analysis of such a wave has been proposed for the determination of material properties of thin films Jia et al. (2018); Wu et al. (2020); Mikhasev et al. (2024). Analyses of surface waves in cylinders with surface/interface energy have been given by Chen et al. (2014); Xu and Fan (2016); Huang (2018); Eremeyev et al. (2020); Mondal et al. (2024); Dhua et al. (2024), where different types of waves and contacts were studied. A generalisation of surface elasticity to surface viscoelasticity with analysis of anti-plane waves was recently given by Eremeyev (2024).

Surface elasticity can be treated as a limiting case of case of nonlocal continuum models Mindlin (1965), see also the comparison between the Mindlin–Toupin strain gradient elasticity and the Gurtin–Murdoch surface elasticity given by Eremeyev et al. (2019), see also Li et al. (2020); Jiang et al. (2022); Yang et al. (2023). Surface waves in nonlocal media have also been studied by Chebakov et al. (2016); Kaplunov et al. (2022).

Another view of surface elasticity could be based on lattice dynamics, see for example the discussion by Murdoch (2005). A scaling law and a certain correspondence between surface elasticity and lattice dynamics has been proposed by Eremeyev and Sharma (2019), where anti-plane waves have also been studied. Using this correspondence the waves in a lattice with a surface defect have been analysed by Sharma and Eremeyev (2019). discrete model Lattice models with non-perfect contact (sliding) have also been discussed by Cabras et al. (2024).

Motivated by the recent contributions, in this contribution we aim to give the detailed analyses of anti-plane shear waves in an elastic plate imperfectly attached to an elastic half-space and study effects of interfacial sliding on the phase velocity of these waves. The remainder of the paper is organised as follows. In Section 1 we give the statement of the problem under consideration in the case of anti-plane motion.Two types of solutions are possible for the plane, expressed by exponential and harmonic (trigonometric) functions, respectively. We call these solutions transverse exponential (TE) and

transverse harmonic (TH). As in (Eremeyev et al., 2016), there are only exponentially decaying solutions for the half-space. A detailed analysis of TE solutions is given in Section 2, while harmonic waves are analysed in Section 3. An exhaustive analysis of the dispersion curves is given in Section 4. Finally, a technique for evaluation a bond stiffness was proposed in Section 5.

1. Statement of the problem

Let us consider an elastic isotropic layer (plate) of thickness h lying on an elastic isotropic half-space with weak interfaces allowing sliding, see Fig. 1.

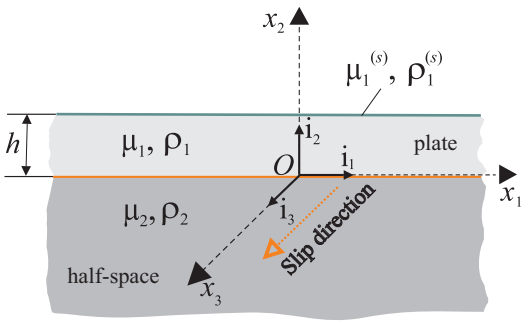

Figure 1: Elastic plate lying on elastic half-space with the interfacial sliding and used Cartesian coordinate system.

For anti-plane waves the vector of displacement $\mathbf{u}$ is assumed in the following form, see *e.g.* Achenbach (1973):

$$\mathbf{u} = \mathbf{u}(x_1, x_2, x_3, t) = u(x_1, x_2, t)\mathbf{i}_3, \tag{1}$$

where t is time and $\mathbf{i}_i$ are the base vectors, $i = 1, 2, 3$, see again Fig. 1.

Assuming that the materials are isotropic, we introduce the shear modulus μ_j and the mass density ρ_j, where the subscripts $j = 1$ and $j = 2$ correspond to the layer and half-space, respectively.

Then the equations of motion for the layer and the half-space take the form of two wave equations (Achenbach, 1973)

$$\mu_j \left(\frac{\partial^2 u_j}{\partial x_1^2} + \frac{\partial^2 u_j}{\partial x_2^2} \right) = \rho_j \frac{\partial^2 u_j}{\partial t^2}, \quad j = 1, 2. \tag{2}$$

Let the upper surface $x_2 = h$ be free. Within the Gurtin-Murdoch model of the surface elasticity, the boundary condition admits the form the compatibility condition (Gurtin and Murdoch, 1975, 1978) and read as:

$$\mu_1 \frac{\partial u_1}{\partial x_2} = \mu_1^{(s)} \frac{\partial^2 u_1}{\partial x_1^2} - \rho_1^{(s)} \frac{\partial^2 u_1}{\partial t^2} \quad \text{at } x_2 = h, \tag{3}$$

where $\mu_1^{(s)}$ and $\rho_1^{(s)}$ are surface shear modulus and mass density, respectively.

At the interface $x_2 = 0$, we assume a sliding with the bond stiffness k_s in the x_3–direction. Then the boundary conditions at the interface are expressed by the following two equations (Newmark, 1951; Gahleitner and Schoeftner, 2021):

$$\mu_1 \frac{\partial u_1}{\partial x_2} = \mu_2 \frac{\partial u_2}{\partial x_2} \qquad \text{at} \quad x_2 = 0, \tag{4}$$

$$\mu_1 \frac{\partial u_1}{\partial x_2} = k_s(u_1 - u_2) \qquad \text{at} \quad x_2 = 0. \tag{5}$$

For the half-space, we consider the wave attenuation condition at infinity:

$$u_2 \longrightarrow 0 \quad \text{as} \quad x_2 \longrightarrow -\infty. \tag{6}$$

Recently it has been shown that if the plate has at least one free surface, then there exist two different regimes (modes) of anti-plane waves, namely the transversely exponential (TE) and the transversely harmonic (TH) regime, see Mikhasev et al. (2022, 2023). In the TE regime, waves decay exponentially from both surfaces of the plate, whereas the TH mode is characterised by waves with harmonic variation of amplitudes in the transverse direction. In the problem under consideration, both TE and TH modes exist in the plate and only the TE regime exists in the half-space. In the following, the possible modes of anti-plane waves in the plate-half-space system will be referred to as TE-TE and TH-TE modes, respectively.

2. TE-TE regime with interfacial sliding

In the TE-TE regime, a solution of Eqs. (2) has the form as in Mikhasev et al. (2023)

$$u_1 = e^{i(kx_1 - \omega t)} \left(a_1 e^{\alpha_1 (x_2 - h_1)} + a_2 e^{-\alpha_1 x_2} \right), \quad u_2 = b e^{i(kx_1 - \omega t)} e^{\alpha_2 x_2}, \tag{7}$$

where $i = \sqrt{-1}$ is the imaginary unit, k is a wave number, ω is a circular frequency, and a_1, a_2, b are constants have to be determined by the boundary conditions.

The substitution of (7) into Eqs. (2) gives

$$\alpha_j = |k|\sqrt{1 - c^2/c_{Tj}^2}, \quad j = 1, 2, \tag{8}$$

where $c = \omega/k$ is the phase velocity, and $c_{Tj} = \sqrt{\mu_j/\rho_j}$ are the shear wave speeds in the upper layer and the half-space for $j = 1$ and $j = 2$, respectively. We assumed that $c < c_{Tj}$ for both $j = 1$, 2.

Applying the boundary conditions (3)–(5) to Eq.(7) and using (8), we get the relations for the constants

$$a_2 = \frac{(\mu_1\alpha_1 - k_s)\mu_2\alpha_2 + \mu_1\alpha_1 k_s}{(\mu_1\alpha_1 + k_s)\mu_2\alpha_2 + \mu_1\alpha_1 k_s} e^{-\alpha_1 h} a_1, \quad b = \frac{\mu_1\alpha_1}{\mu_2\alpha_2}\left(a_1 e^{-\alpha_1 h} - a_2\right) \tag{9}$$

and the required dispersion equation became

$$\begin{aligned} &c_{T1}^2\sqrt{1 - \frac{c^2}{c_{T1}^2}}\left[l_d|k|\left(c^2 - c_s^2\right)\right]^{-1} \\ &= \frac{(\mu_1\alpha_1 + k_s)\mu_2\alpha_2 + \mu_1\alpha_1 k_s + e^{-2\alpha_1 h}\left[(\mu_1\alpha_1 - k_s)\mu_2\alpha_2 + \mu_1\alpha_1 k_s\right]}{(\mu_1\alpha_1 + k_s)\mu_2\alpha_2 + \mu_1\alpha_1 k_s - e^{-2\alpha_1 h}\left[(\mu_1\alpha_1 - k_s)\mu_2\alpha_2 + \mu_1\alpha_1 k_s\right]} \end{aligned} \tag{10}$$

where $c_s = \sqrt{\mu_1^{(s)}/\rho_1^{(s)}}$ is a shear wave speed in an elastic membrane associated with the Gurtin–Murdoch model, and $l_d = \rho_1^{(s)}/\rho_1$ is the so-called dynamic characteristic length-scale parameter.

Introducing the dimensionless quantities

$$m_{12} = \frac{\mu_1}{\mu_2}, \quad k_d = |k|l_d, \quad n = \frac{h}{l_d}, \quad \kappa_s = \frac{\mu_1\rho_1}{k_s\rho_1^{(s)}} \tag{11}$$

and scaling of velocities

$$v = \frac{c}{c_{T1}}, \quad v_s = \frac{c_s}{c_{T1}}, \quad v_r = \frac{c_{T2}}{c_{T1}}, \tag{12}$$

we can rewrite the dispersion equation (10) in the dimensionless form

$$\frac{R_{EE} - 1}{R_{EE} + 1} = \frac{k_d(v^2 - v_s^2)}{\sqrt{1 - v^2}} \tag{13}$$

with

$$R_{EE} = \frac{\sqrt{1-v^2}\left[k_d\kappa_s\sqrt{1-\frac{v^2}{v_r^2}}+m_{12}\right]+\sqrt{1-\frac{v^2}{v_r^2}}}{\sqrt{1-v^2}\left[k_d\kappa_s\sqrt{1-\frac{v^2}{v_r^2}}+m_{12}\right]-\sqrt{1-\frac{v^2}{v_r^2}}}\times e^{2nk_d\sqrt{1-v^2}}. \tag{14}$$

It can be seen that for the TE-TE mode $v < 1$, i.e. for any parameter κ_s the velocity of anti-plane waves is less than the velocity of shear waves in the plate.

The dispersion relation (13) allows us to consider several special cases, especially those already analysed in the literature. Thus, assuming $m_{12} = 0$ in (14) for $0 < k_s < \infty$, we obtain the new equation (13) for the plate attached to the non-deformable half-space with an elastic constraint for shear at the bottom.

If $\kappa_s = 0$ (i.e., $k_s \to \infty$), we came to the equation for the plate rigidly attached to the elastic half-space studied by Mikhasev et al. (2023):

$$\left(\sqrt{1-\frac{v^2}{v_r^2}}+m_{12}\sqrt{1-v^2}\right)\left(\frac{1}{k_d}\sqrt{1-v^2}+v_s^2-v^2\right)$$
$$+\left(\sqrt{1-\frac{v^2}{v_r^2}}-m_{12}\sqrt{1-v^2}\right)\left(\frac{1}{k_d}\sqrt{1-v^2}-v_s^2+v^2\right)e^{-2nk_d\sqrt{1-v^2}}=0. \tag{15}$$

When either $m_{12} \to \infty$ or $\kappa_s \to \infty$ (i.e., $\mu_2 \to 0$ or $k_s \to 0$), Eq. (13) degenerates into the equation (compare with Eq. (3.15) in Mikhasev et al. (2022))

$$\frac{1}{k_d}\sqrt{1-v^2}+v_s^2-v^2-\left(\frac{1}{k_d}\sqrt{1-v^2}-v_s^2+v^2\right)e^{-2nk_d\sqrt{1-v^2}}=0, \tag{16}$$

which corresponds to the plate with free bottom surface without the surface stresses.

If $m_{12} = \kappa_s = 0$ (i.e., $\mu_2 \to \infty$ and $k_s \to \infty$), then we arrive at the dispersion equation for the plate (single layer) with the bottom surface $x_2 = 0$ rigidly clamped in the x_3-direction, see Eq. (3.7) in Mikhasev et al. (2022)

$$\frac{1}{k_d}\sqrt{1-v^2}+v_s^2-v^2+\left(\frac{1}{k_d}\sqrt{1-v^2}-v_s^2+v^2\right)e^{-2nk_d\sqrt{1-v^2}}=0. \tag{17}$$

Passing to the limit as $n \to \infty$ (or $h \to \infty$), we get the simple dispersion equation Eremeyev and Sharma (2019))

$$\frac{1}{k_d}\sqrt{1-v^2} + v_s^2 - v^2 = 0 \tag{18}$$

for the half-space with shear modulus μ_1 and density ρ_1.

Finally, assuming $n = 0$ (or $h = 0$) and returning to the initial dimensional variables, we arrive at the following new dispersion equation:

$$\frac{k_s\sqrt{1-\frac{c^2}{c_{T2}^2}}}{k_s + |k|\mu_2\sqrt{1-\frac{c^2}{c_{T2}^2}}} = |k|\frac{\rho_1^{(s)}}{\rho_2}\left(\frac{c^2}{c_{T2}^2} - \frac{c_s^2}{c_{T2}^2}\right). \tag{19}$$

This equation describes anti-plane shear waves in the elastic half-space with the shear modulus μ_2 and density ρ_2, which is covered by the nanofilm (nanomembrane) with $\mu^{(s)} = \mu_1^{(s)}, \rho^{(s)}$, this film allowing elastic sliding along the surface. Substituting . Considering the limit as $k_s \to \infty$ in (19), we again arrive at Eq. (18), but for the half-space with parameters μ_2, ρ_2.

Remark. The dispersion equation (19) deserves special consideration: it could be treated as follows. Let u_m be the displacements of the film in the x_3-direction, and u_2 is the displacement of the half-space, which differ from u_m for $x_2 = 0$, in general. The relative displacement $u_m - u_2$ results in the shear stress $S = k_s(u_m - u_2)$ on the half-space surface, where k_s is the bond stiffness (Newmark, 1951). Then the differential equation governing the anti-plane waves in the "half-space–sliding nanofilm" system is

$$\mu^{(s)}\frac{\partial^2 u_m}{\partial x_1^2} - \rho^{(s)}\frac{\partial^2 u_m}{\partial t^2} = k_s(u_m - u_2), \tag{20}$$

and the equation for the half-space remains the same, i.e. Eq. (2) with $j = 2$.

The boundary condition for the half-space coated with the film will is given by

$$\mu_2\frac{\partial u_2}{\partial x_2} = k_s(u_m - u_2) \quad \text{for} \quad x_2 = 0. \tag{21}$$

Looking for the displacement of the film as $u_m = a_m e^{i(kx_1 - \omega t)}$, where a_m is an arbitrary constant, and substituting it together with the ansatz (7) for u_2 into Eqs. (2), (20), and the boundary condition (21), we obtain the dispersion equation (19). In particular, for $k_s = 0$ this equation gives the velocity of shear waves in the film, $c = c_s = \sqrt{\mu^{(s)}/\rho^{(s)}}$.

3. TH-TE regime with interfacial sliding

Let us now consider the second solution, i.e. the TH-TE regime for with solutions of Eqs. (2) assumed in the form (Mikhasev et al., 2023):

$$u_1 = e^{i(kx_1-\omega t)}\left(a_1 \sin \lambda x_2 + a_2 \cos \lambda x_2\right), \quad u_2 = be^{i(kx_1-\omega t)}e^{\alpha x_2}, \tag{22}$$

where a_1, a_2, b are constants.

Substituting (22) into Eqs. (2) we get

$$\lambda = |k|\sqrt{\frac{c^2}{c_{T1}^2}-1}, \quad \alpha = |k|\sqrt{1-\frac{c^2}{c_{T2}^2}} \tag{23}$$

with $c_{T1} < c < c_{T2}$.

Substitution of (22) into the boundary conditions (3)–(5) gives us the coupling constants

$$b = \frac{\mu_1}{\mu_2}\frac{\lambda}{\alpha}a_1, \quad a_2 = \frac{\mu_1\lambda(\alpha\mu_2+k_s)}{k_s\alpha\mu_2}a_1, \tag{24}$$

and the required dispersion equation for TH-TE becomes

$$\frac{|k|l_d(v^2-v_s^2)}{\sqrt{v^2-1}} = \frac{k_s\alpha\mu_2\cos\lambda h - \lambda(\alpha\mu_1\mu_2+k_s\mu_1)\sin\lambda h}{k_s\alpha\mu_2\cos\lambda h + \lambda(\alpha\mu_1\mu_2+k_s\mu_1)\sin\lambda h}. \tag{25}$$

The dimensionless form of (25) is given by

$$\frac{1-R_{HE}\tan\left(nk_d\sqrt{v^2-1}\right)}{\tan\left(nk_d\sqrt{v^2-1}\right)+R_{HE}} = \frac{k_d(v^2-v_s^2)}{\sqrt{v^2-1}} \tag{26}$$

with

$$R_{HE} = \frac{\sqrt{v^2-1}\left(k_d\kappa_s\sqrt{1-\frac{v^2}{v_r^2}}+m_{12}\right)}{\sqrt{1-\frac{v^2}{v_r^2}}}. \tag{27}$$

Note that here $1 < v < v_r$, i.e. $c_{T1} < c < c_{T2}$.

Similar to the TE-TE regime analysed in the previous section, Eq. (26) possesses derivation of the dispersion relations for some particular cases.

For example, if $\kappa_s = 0$, we obtain the TE-TH regime dispersion equation for the layer rigidly attached to the half-space (see Eq. (20) in Mikhasev et al. (2023)).

If $m_{12} = 0$ and $0 < \kappa_s < \infty$, then we get the new TE-TH regime equation for the plate which can slide along the non-deformable half-space

$$\frac{1 - k_d\kappa_s\sqrt{v^2-1}\,\tan(nk_d\sqrt{v^2-1})}{\tan(nk_d\sqrt{v^2-1}) + k_d\kappa_s\sqrt{v^2-1}} = \frac{k_d\,(v^2 - v_s^2)}{\sqrt{v^2-1}}. \tag{28}$$

Assuming $m_{12} = 0$ and $\kappa_s = 0$, we get the relatively simple equation for the TH regime in an elastic layer with clamped bottom face in the x_3–direction, see Eq. (3.10) in Mikhasev et al. (2022).

When $m_{12} \to \infty$ or $\kappa_s \to \infty$, then Eq. (26) degenerates into the equation for TH regime in an elastic layer with free bottom face without any surface effects at it, see Eq. (29) in Mikhasev et al. (2023).

Finally, letting the plate thickness vanish, i.e. $n \to 0$, we arrive at the equation, which has not any solution. So in this case we have not propagating anti-plane waves.

4. Dispersion curves analysis

Let us discuss the dispersion relations for all modes in more detail.

4.1. TE-TE regime

We start our analysis with Eq. (13), which relates to the TE-TE regime. First, note that the value $v = 1$ should be excluded because it is only the trivial solution of Eqs. (2), see relations (7)-(9). Second, the case wh n $v_s \geq 1$ should also be excluded, since there are no TE-TE mode antiplane waves if $c_s \geq c_{T1}$ (Eremeyev and Sharma, 2019).

We begin our analysis with Eq. (13) related to the TE-TE regime. First, let us note that the value $v = 1$ should be excluded, because it is just the trivial solution to the wave Eqs. (2), see relations (7)-(9). Secondly, the case $v_s \geq 1$ should be also excluded, since there are no TE-TE mode anti-plane waves if $c_s \geq c_{T1}$ (Eremeyev and Sharma, 2019).

A numerical analysis shows that there are two different cases in which the behaviour of the dispersion curves is fundamentally different.

Let $v_r > 1$, i.e. the velocity of the shear waves in the half-space is greater than the velocity of the shear waves in the plate.

Figure 2 displays the dimensionless phase velocity $v = c/c_{T1}$ versus the dimensionless wave parameter $k_d = |k|l_d$ calculated at the following values: $v_r = 2$, $v_s = 0.25$, $m_{12} = 0.5$, $n = 5.5$, and for different values of $\kappa_s =$

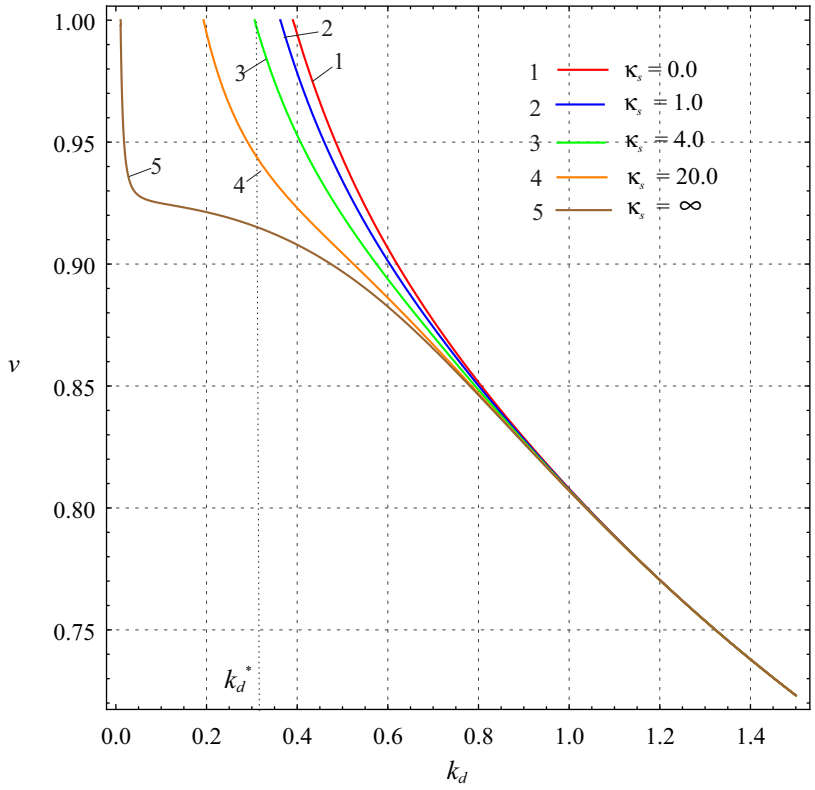

Figure 2: Dimensionless phase velocity $v = c/c_{T1}$ for TE-TE regime *vs.* wave number $k_d = |k|l_d$ calculated at $v_r = 2$, $v_s = 0.25$, $m_{12} = 0.5$, $n = 5.5$ for different values of the dimensionless parameter κ_s: red, blue, green, orange and brown curves marked by 1, 2, 3, 4 and 5 correspond to ratios $\kappa_s = 0$, 1, 4, 20 and ∞, respectively.

0, 1, 4, 20, ∞. The red curve 1 ($\kappa_s = 0$) is related to the case when the contact between the plate and half-space is rigid, while the brown curve 5 ($\kappa_s = \infty$) corresponds to the plate with the free lower surface. We can see that all dispersion curves at $0 < \kappa_s < \infty$ lie between curves 1 and 5. Any dispersion curve begins at the point $(k_d^*, 1)$, which is to be excluded, and then goes down as k_d increases. At $k_d \to \infty$, all curves approaches the straight horizontal line $v = v_s$ (here $v_s = 0.25$). The behaviour of the dispersion curve in the neighbourhood of the point $(k_d^*, 1)$ can be approximated by the linear function

$$v = 1 - A(k_d - k_d^*) + O\left[(k_d - k_d^*)^2\right] \quad \text{as} \quad k_d \longrightarrow k_d^*. \tag{29}$$

The substitution of (29) into (13) results in equations for k_d^*, A. In particular,

we obtain

$$k_d^* = \frac{\sqrt{m_{12}^2(1-v_s^2)^2 v_r^2 + 4(n+\kappa_s)(1-v_s^2)(v_r^2-1)} - m_{12}(1-v_s^2)v_r}{2(n+\kappa_s)(1-v_s^2)\sqrt{v_r^2-1}}. \quad (30)$$

The relation for A is rather awkward and not given here.

If $\kappa_s = 0$ (or $k_s = \infty$), then (30) coincides with formula (31) derived by Mikhasev et al. (2023) for the case of perfect contact between a plate and an elastic isotropic half-space. The deviation of k_d^* from the value $k_d^*|_{\kappa_s=0}$ can be used as a criterion for assessing the bond strength between a thin plate and a more rigid elastic body. The greater the deviation, the weaker the bond at the interface.

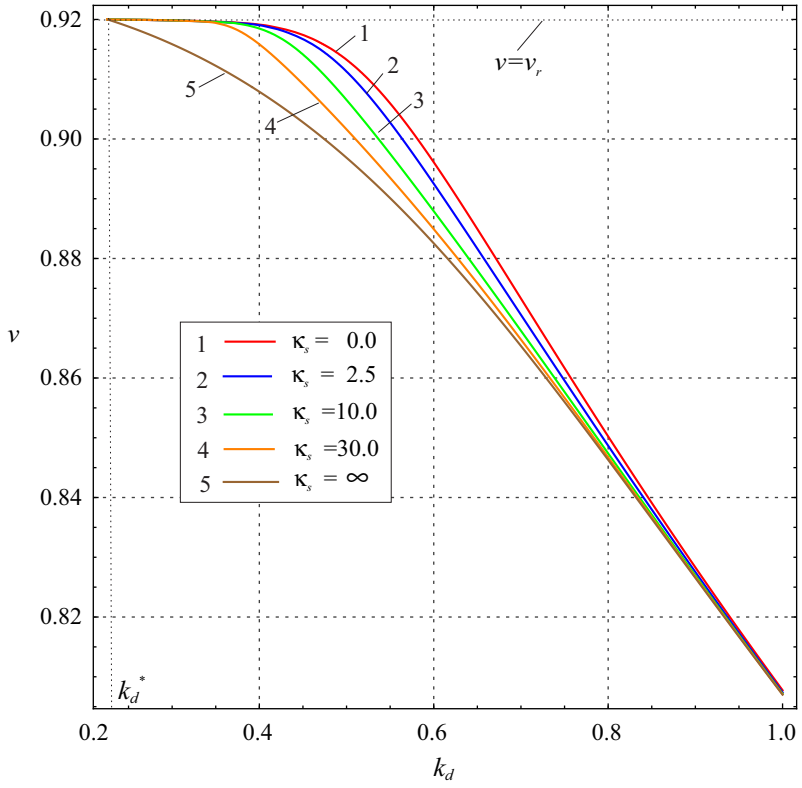

Figure 3: Dimensionless phase velocity $v = c/c_{T1}$ for TE-TE regime *vs.* wave number $k_d = |k|l_d$ calculated at $v_r = 0.92$, $v_s = 0.25$, $m_{12} = 0.5$, $n = 5.5$ for different values of the dimensionless parameter κ_s: red, blue, green, orange and brown curves marked by 1, 2, 3, 4 and 5 correspond to ratios $\kappa_s = 0$, 2.5, 10, 30 and ∞, respectively.

Now, let $v_s < v_r \leq 1$ (i.e., $c_s < c_{T2} \leq c_{T1}$). The plots in Fig. 3 show the

behaviour of dispersion curves for $v_r = 0.92$, $v_s = 0.25$, $m_{12} = 0.5$, $n = 5.5$, and $\kappa_s = 0$, 2.5, 10, 30, ∞. It is seen that here all the dispersion curves begin at the point (k_d^*, v_r) independently on the bond stiffness between the plate and the half-space. Their behaviour near this point can be approximated by the asymptotic relation

$$v = v_r - A(k_d - k_d^*)^2 + O\left[(k_d - k_d^*)^3\right] \quad \text{as} \quad k_d \longrightarrow k_d^*. \tag{31}$$

Substituting (31) into (13) and considering the first two approximations, we arrive at the transcendental equation

$$\tanh\left(nk_d^*\sqrt{1-v_r^2}\right) = \frac{k_d^*(v_r^2 - v_s^2)}{\sqrt{1-v_r^2}} \tag{32}$$

with respect to k_d^*, and at the following equation for determination of the coefficient A:

$$\begin{aligned} &\frac{\mathrm{e}^{2nk^*\sqrt{1-v_r^2}}}{m_{12}}\left[\sqrt{\frac{2A}{v_r}}\left(1 + k_d^*\kappa_s\sqrt{1-v_r^2} - \frac{k_d^*\kappa_s\sqrt{1-v_r^2}-1}{m_{12}\sqrt{1-v_r^2}}\right)\right. \\ &\left.+2nm_{12}(1-v_r^2)\right]\left[1 - \frac{k_d^*(v_r^2-v_s^2)}{\sqrt{1-v_r^2}}\right] = (v_r^2 - v_s^2)\left(\mathrm{e}^{2nk^*\sqrt{1-v_r^2}} + 1\right). \end{aligned} \tag{33}$$

Equation (32) has a nontrivial solution if and only if $v_s < v_r < 1$. When $v_r = 1$, then $k_d^* = 0$.

Figure 4 displays the dispersion curves plotted for $\kappa_s = 4$, $v_s = 0.25$, $m_{12} = 0.5$, $n = 5.5$, and different dimensionless ratios v_r, including both cases where $v_s < v_r \leq 1$ and $v_r > 1$. It can be seen that the behaviour of the dispersion curves in the vicinity of the points (k_d^*, v_r) and $(k_d^*, 1)$ for these cases is different. However, all curves almost merge with growths of k_d, i.e. they asymptotically approaches the horizontal line $v = v_s$.

4.2. TH-TE regime

Let us now analyse the dispersion curves corresponding to TH-TE regime. We recall that for these modes $1 < v < v_r$. Here, there are two fundamentally different variants depending on the position of v_s with respect to the segment $[1, v_r]$. The solutions of Eq. (26) versus k_d are presented in Fig. 5 for the case $v_s < 1$. Computations were done at $v_r = 2$, $v_s = 0.25$, $m_{12} = 0.5$, $n = 5.5$,

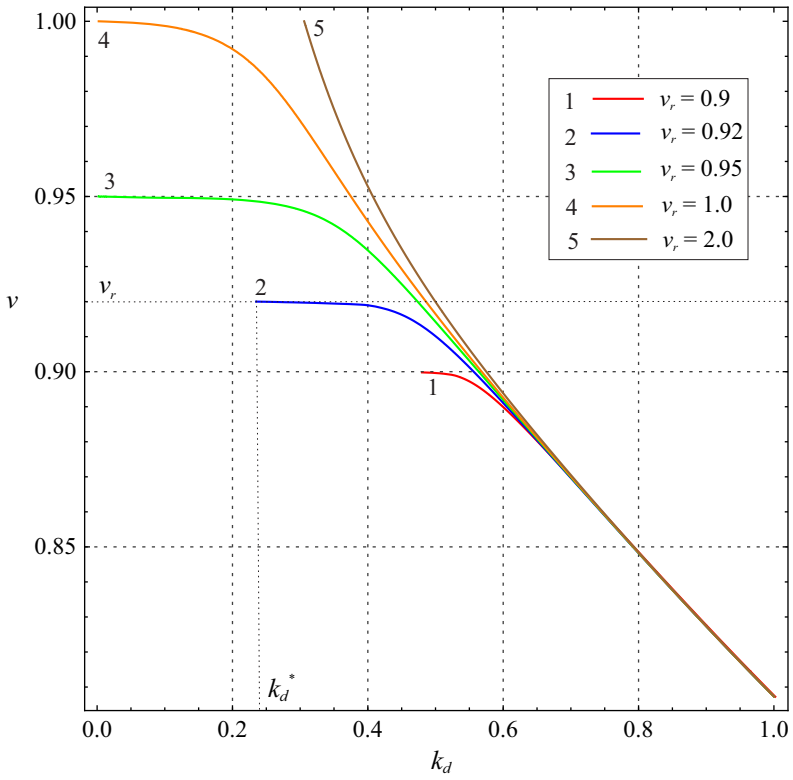

Figure 4: Dimensionless phase velocity $v = c/c_{T1}$ for TE-TE regime *vs.* wave number $k_d = |k|l_d$ calculated at $\kappa_s = 4$, $v_s = 0.25$, $m_{12} = 0.5$, $n = 5.5$ for different values of the dimensionless ratio v_r: red, blue, green, orange and brown curves marked by 1, 2, 3, 4 and 5 correspond to ratios $v_r = 0.9$, 0.92, 0.95, 1 and 2, respectively.

and for different values of the dimensionless parameter κ_s. This mode of anti-plane waves is characterized by the presence of an infinite number of branches of dispersion curve. It is interest to note, that if $v_s < 1$, then there exists the branch (left-hand one) crossing the line $v = 1$, which is a continuation of the dispersion curve corresponding to the TE-TE regime plotted for the same input parameters, see Fig. 2. If $v_s > 1$, then this branch is absent. In Figure 6, the dispersion curves are depicted for different $1 < v_s < v_r$ with the same input parameters v_r, κ_s, n, m_{12} as in Fig. 5. Since plots of dispersion curves for $v_s \geq v_r$ are approximately the same as the plots shown in Fig. 6, we do not present them here.

Independently on ratios between the material parameters, any of the dispersion curve related to the TH-TE regime begins at the point (k_d^*, v_v) which

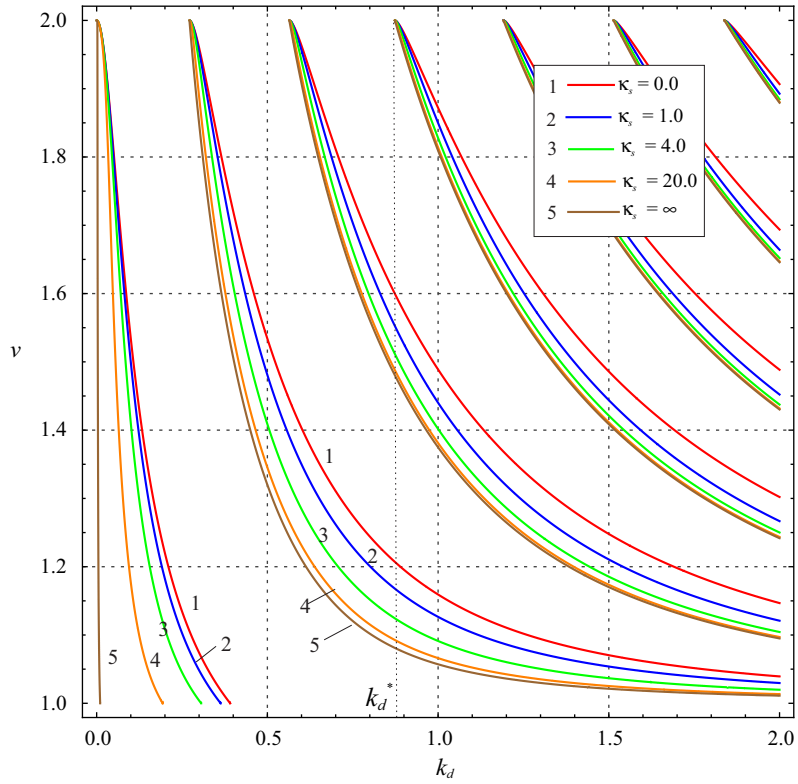

Figure 5: Dimensionless phase velocity $v = c/c_{T1}$ for TH-TE regime *vs.* wave number $k_d = |k|l_d$ evaluated at $v_r = 2$, $v_s = 0.25$, $m_{12} = 0.5$, $n = 5.5$ and for different dimensionless parameters κ_s: red, blue, green, orange, and brown curves marked by 1, 2, 3, 4 and 5 correspond to ratios $\kappa_s = 0$, 1, 4, 20 and ∞, respectively.

is excluded. In the vicinity of the point k_d, the phase velocity $v(k_d)$ can be approximated by the function

$$v = v_r - A\sqrt{k_d - k_d^*} + O(k_d - k_d^*) \quad \text{as} \quad k_d \longrightarrow k_d^*, \tag{34}$$

where k_d^* is determined from the following equation

$$\tan\left(nk_d^*\sqrt{v_r^2 - 1}\right) = \frac{k_d^*(v_s^2 - v_r^2)}{\sqrt{(v_r^2 - 1)}}. \tag{35}$$

The latter coincides with Eq. (33) obtained by Mikhasev et al. (2023) for the plate rigidly attached to the half-space. Thus, for the TH-TE modes of anti-plane waves, the parameter k_d^* is independent of the bond stiffness at the interface.

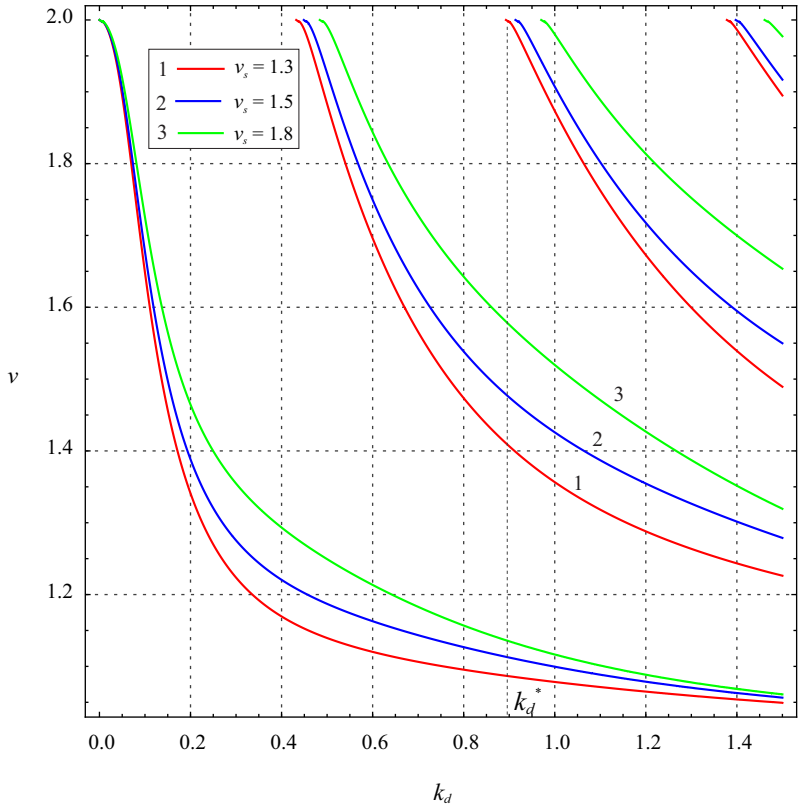

Figure 6: Dimensionless phase velocity $v = c/c_{T1}$ for TH-TE regime *vs.* wave number $k_d = |k|l_d$ evaluated at $v_r = 2$, $\kappa_s = 4$, $m_{12} = 0.5$, $n = 5.5$ for different dimensionless ratio $v_s = 1.3, 1.5, 1.8$: red, blue, green curves marked by 1, 2, 3, respectively.

4.3. Anti-plane shear waves in elastic half-space coated with sliding film

Let us consider the case without the plate, i.e. $n = 0$. Then the half-space with the attached plate is transformed into the elastic half-space imperfectly coated by an elastic film (or membrane) which possesses sliding along the interface. The corresponding dispersion equation (19) can be rewritten in the dimensionless form as follows

$$\frac{\sqrt{1-v^2}}{1+k_d\kappa_s\sqrt{1-v^2}} = k_d(v^2 - v_s^2) \tag{36}$$

with the dimensionless velocity $v = c/c_{T2}$ and the new ratios

$$v_s = \frac{c_s}{c_{T2}}, \quad \kappa_s = \frac{\mu_2\rho_2}{k_s\rho_1^{(s)}}, \quad k_d = \frac{\rho_1^{(s)}}{\rho_2}|k|. \tag{37}$$

Here $v_s \le v < 1$, i.e., $c_s \le c < c_{T2}$.

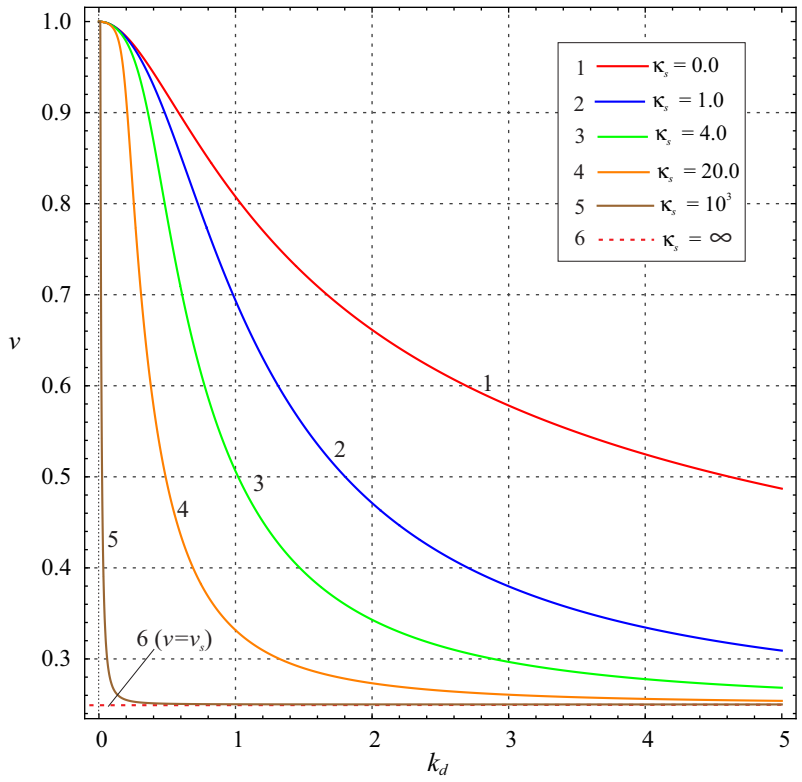

Figure 7: Dimensionless phase velocity $v = c/c_{T2}$ of shear waves in the half-space coated with the film *vs.* wave number $k_d = |k|l_d$ for different dimensionless parameter κ_s evaluated at $v_s = 0.25$: the red, blue, green, orange and brown curves marked by 1, 2, 3, 4 and 5 correspond to the ratios $\kappa_s = 0$, 1, 4, 20 and 10^3, respectively; the red dashed straight line marked by 6 is related to $\kappa_s = \infty$.

Figure 7 displays the solution of Eq. (36) with respect to v as a function of the wave parameter k_d at $v_s = 0.25$, and for different values of $\kappa_s = 0.0, 1.0, 4.0, 20.0$ and 10^3. The red dashed curve 6 is related to the case when the film surface is free ($\kappa_s = \infty$). For any κ_s, all dispersion curves begin at the point $(0, 1)$.. Near this point the phase velocity can be approximated by the following function

$$v = 1 - A_2 k_d - A_4 k_d^4 + O(k_d^6) \quad \text{as} \qquad k_d \to 0, \tag{38}$$

where $A_2 > 0$. Substituting (38) into Eq. (36) and equating coefficients by

k_d and k_d^3, we get the following relations:

$$A_2 = \frac{1}{2}(1 - v_s^2), \quad -\frac{\sqrt{2A_2}()A_2^2 + 2A_4}{4A_2} = (1 - v_s^2)\sqrt{2A}\kappa_s - A_2. \tag{39}$$

It can be seen from Fig. 7 that the dispersion curves plotted for $0 < \kappa_s < \infty$ lie between curve 1 and line 6, corresponding to shear waves in half-space with the film perfectly bonded to its surface and shear waves in the film, respectively. An increase in the parameter κ_s (i.e. a decrease in the bond stiffness k_s) leads to a decrease in the phase velocity of the anti-plane shear waves. When $k_d \to \infty$, all dispersion curves approach the red dashed line 6 for which $v = v_s$ (here $v_s = 0.25$). Note the strong influence of the bond stiffness k_s on the dispersion curves. A significant decrease in the phase velocity of the anti-plane shear waves in the half-space covered by the nanofilm, compared to the value taken in the red curve 1, can be considered as a sign of weakening of the bond between the film and the half-space.

Similar dispersion curves for $\kappa_s = 4$ and different $v_s = 0.02$, 0.3, 0.5, 0.7, 0.9 are shown in Fig. 8. As can be seen, the phase velocity of the anti-plane shear waves in the half-space covered by the sliding film increases together with the velocity c_s of the shear waves in this film, and the dispersion curve approaches the straight line $v = 1(c = c_{T2})$ as $c_s \to c_{T2}$.

5. Towards assessment of bond stiffness

The above derived equations for the lower bounds of the dimensionless wave parameter k_d^* can be used for the experimental evaluation of the bond stiffness at the interface. For this purpose, the TE-TE mode of the antiplane waves, which propagate at a lower speed than the TH-TE mode waves, seems to be more useful.

5.1. Soft plate attached to stiffer half-space

Let us consider the case where the velocity of the shear waves in the half-space is greater than that in the plate, i.e. $v_r > 1$. Such a case can occur when the plate is softer than the half-space, and it is the simplest for estimating the bond strength, since here one can use the relation (30) which contains the dimensionless parameter κ_s in the explicit form. It can also be seen from Fig.2 that each different value of the bond stiffness correlates with a unique phase velocity when the dimensionless wavenumber k_d approaches the value k_d^*.

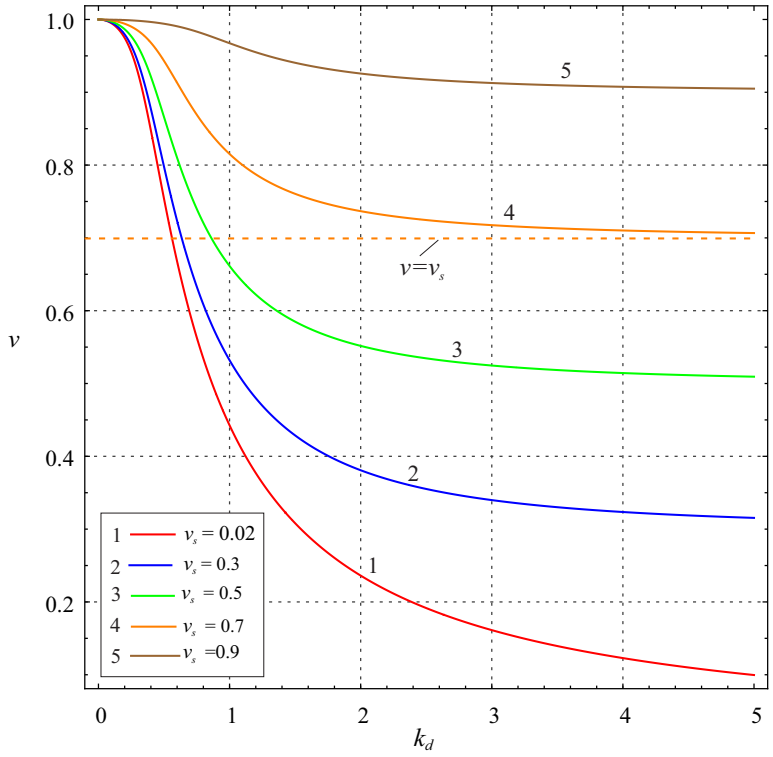

Figure 8: Dimensionless phase velocity $v = c/c_{T2}$ of shear waves in the half-space coated with the film *vs.* wave number $k_d = |k|l_d$ for different dimensionless parameter v_s evaluated at $\kappa_s = 4$: red, blue, green, orange and brown curves marked by 1, 2, 3, 4 and 5 correspond to ratios $v_s = 0.02$, 0.3, 0.5, 0.7 and 0.9, respectively.

The procedure for the experimental estimation of the parameter κ_s could be organised as follows. One has to carry out the series of experiments exciting anti-plane waves with different wave numbers k until the phase velocity $v < 1$ is as close to unity as possible, see Fig. 2. The corresponding dimensionless wave parameter k_d is assigned as the required value k_d^*. Then, knowing all the input parameters, including the shear modulus $\mu_1^{(s)}$ and the density $\rho_1^{(s)}$, an approximate value κ_s can be calculated from Eq. (30).

5.2. Stiffer plate attached to softer half-space

Let $v_r < 1$, i.e. $c_{T1} > c_{T2}$. This case is more difficult to estimate the bond stiffness because the dispersion curves corresponding to different parameters κ_s (see Fig. 3) merge as the dimensionless wave number k_d approaches the same value k_d^*. Nevertheless, the procedure for finding the bond stiffness can

also be developed here. It consists of three steps. First, after knowing all the mechanical properties for the half-space and the plate, including the surface properties, we solve Eq. (32) to find the dimensionless wavenumber k_d^*. In the second step, we perform experiments to measure the dimensionless phase velocity v for the wavenumbers $k_d > k_d^*$ from the right neighbourhood of the point k_d^*. Then, using Eq. (31), we can calculate the coefficient A. Finally, using Eq. (33) and taking into account Eq. (32), we find the value of the dimensionless parameter κ_s:

$$\kappa_s = \frac{m_{12}}{k_d^*(m_{12}-1)}\sqrt{\frac{v_r}{2A}}\left[\frac{m_{12}\sqrt{1-v_r^2}}{k_d^*}\sinh\left(2nk_d^*\sqrt{1-v_r^2}\right)\right.$$
$$\left.-\sqrt{\frac{2A}{v_r}}\left(1+\frac{1}{m_{12}\sqrt{1-v_r^2}}\right)-2nm_{12}(1-v_r^2)\right]. \tag{40}$$

5.3. Half-space coated by a film

For the elastic half-space covered by the sliding film, the procedure for evaluating the parameter κ_s could be constructed as follows. First, using Eq. $(39)_1$, we calculate A_2. Then, by performing experiments and measuring the velocity v at a very low frequency, as k_d tends to zero, we calculate A_4 from Eq. (38). Finally, using Eq. $(39)_2$, we can find the required parameter

$$\kappa_s = \frac{4(1-v_s^2)^3 + 8A_4 - (1-v_s^2)^4}{8(1-v_s^2)^3}, \tag{41}$$

which is positive if $A_4 > 0$.

Conclusions

We have provided a detailed analysis of anti-plane motions in the "plate-half-space" elastic system, considering both surface stresses on the free surface and possible sliding between the plate and half-space. The surface stresses have been modelled within the linear Gurtin-Murdoch model of surface elasticity. To describe the sliding, a linear spring-like model is introduced so that the interfacial shear stresses are a linear function of the relative displacements of the plate and the half-space with a coefficient called the bond stiffness. New dispersion equations taking into account the surface energy and interfacial sliding for two different regimes of anti-plane waves have been

derived. The first type of anti-plane waves, called the TE-TE regime, is characterised by the exponentially decaying amplitudes from the top and interface surfaces in both the plate and half-space. The second class of waves, called the TH-TE regime, is specified by the harmonic (trigonometric) variation of the amplitudes in the plate and the exponential decay of the waves in the half-space bulk. As a limit case, we obtained the dispersion equation for anti-plane waves in the elastic half-space covered by the film, which possesses sliding. This case refers to the absence of the plate.

The analysis of the dispersion curves showed a significant influence of the interfacial bond stiffness on the phase velocities. It consists in the decrease of the phase velocities with the weakening of the interfacial bonds. The more pronounced effect of interfacial sliding on the phase velocities was observed for the long-length waves belonging to the TE-TE regime. It is interesting to note that this effect is stronger when the shear wave velocity in the plate is lower than the shear wave velocity in half space, and less pronounced otherwise. We also derived the asymptotic relations for lower bounds on the wave number from which anti-plane shear waves exist, and found functions approximating the phase velocities in the vicinity of these bounds. Based on the derived equations for the lower bounds of the wave numbers, we proposed an evaluation technique for the bond stiffness in thin plates imperfectly attached to an elastic half-space. Thus, the obtained results could be used for non-destructive evaluation of debonding phenomena in solids with coatings.

Acknowledgments

G.I.M. acknowledges the support from the Harbin Institute of Technology, China, within the framework of the start-up research grant. V.A.E. acknowledges the support within the project "Metamaterials design and synthesis with applications to infrastructure engineering" funded by the MUR Progetti di Ricerca di Rilevante Interesse Nazionale (PRIN) Bando 2022 - grant 20228CPHN5, Italy, and the support of the European Union's Horizon 2020 research and innovation program under the RISE MSCA EffectFact Project agreement No 101008140.

Data availability

Data will be made available on request.

Declaration of competing interest

The authors declare that they have no known competing financial interests or personal relationships that could have appeared to influence the work reported in this paper.

References

References

Achenbach, J., 1973. Wave Propagation in Elastic Solids. North Holland, Amsterdam.

Brekhovskikh, L.M., 1960. Waves in Layered Media. Academic Press, New York.

Cabras, L., Bigoni, D., Piccolroaz, A., 2024. Dynamics of elastic lattices with sliding constraints. Proceedings of the Royal Society A 480, 20230579.

Chebakov, R., Kaplunov, J., Rogerson, G.A., 2016. Refined boundary conditions on the free surface of an elastic half-space taking into account nonlocal effects. Proceedings of the Royal Society A: Mathematical, Physical and Engineering Sciences 472, 20150800.

Chen, W.Q., Wu, B., Zhang, C.L., Zhang, C., 2014. On wave propagation in anisotropic elastic cylinders at nanoscale: surface elasticity and its effect. Acta Mechanica 225, 2743–2760.

Dhua, S., Maji, A., Nath, A., 2024. The influence of surface elasticity on shear wave propagation in a cylindrical layer structure with an imperfect interface. European Journal of Mechanics-A/Solids 106, 105318.

Duan, H.L., Wang, J., Karihaloo, B.L., 2008. Theory of elasticity at the nanoscale, in: Advances in Applied Mechanics. Elsevier. volume 42, pp. 1–68.

Eremeyev, V.A., 2016. On effective properties of materials at the nano- and microscales considering surface effects. Acta Mechanica 227, 29–42.

Eremeyev, V.A., 2020. Strongly anisotropic surface elasticity and antiplane surface waves. Philosophical Transactions of the Royal Society A 378, 20190100.

Eremeyev, V.A., 2024. Surface finite viscoelasticity and surface anti-plane waves. International Journal of Engineering Science 196, 104029.

Eremeyev, V.A., Rosi, G., Naili, S., 2016. Surface/interfacial anti-plane waves in solids with surface energy. Mechanics Research Communications 74, 8–13.

Eremeyev, V.A., Rosi, G., Naili, S., 2019. Comparison of anti-plane surface waves in strain-gradient materials and materials with surface stresses. Mathematics and Mechanics of Solids 24, 2526–2535.

Eremeyev, V.A., Rosi, G., Naili, S., 2020. Transverse surface waves on a cylindrical surface with coating. International Journal of Engineering Science 147, 103188.

Eremeyev, V.A., Rosi, G., Naili, S., 2024. On effective surface elastic moduli for microstructured strongly anisotropic coatings. International Journal of Engineering Science , submitted.

Eremeyev, V.A., Sharma, B.L., 2019. Anti-plane surface waves in media with surface structure: Discrete vs. continuum model. International Journal of Engineering Science 143, 33–38.

Ewing, W.M., Jardetzky, W.S., Press, F., 1957. Elastic Waves in Layered Media. McGraw-Hill Book Company, New York.

Gahleitner, J., Schoeftner, J., 2021. A two-layer beam model with interlayer slip based on two-dimensional elasticity. Composite Structures 274, 114283.

Gorbushin, N., Eremeyev, V.A., Mishuris, G., 2020. On stress singularity near the tip of a crack with surface stresses. International Journal of Engineering Science 146, 103183.

Gurtin, M.E., Murdoch, A.I., 1975. A continuum theory of elastic material surfaces. Archive for Rationional mechanics and Analysis 57, 291–323.

Gurtin, M.E., Murdoch, A.I., 1978. Surface stress in solids. International Journal of Solids and Structures 14, 431–440.

Huang, Z., 2018. Torsional wave and vibration subjected to constraint of surface elasticity. Acta Mechanica 229, 1171–1182.

Javili, A., McBride, A., Steinmann, P., 2013. Thermomechanics of solids with lower-dimensional energetics: on the importance of surface, interface, and curve structures at the nanoscale. A unifying review. Applied Mechanics Reviews 65, 010802.

Jia, F., Zhang, Z., Zhang, H., Feng, X.Q., Gu, B., 2018. Shear horizontal wave dispersion in nanolayers with surface effects and determination of surface elastic constants. Thin Solid Films 645, 134–138.

Jiang, Y., Li, L., Hu, Y., 2022. A nonlocal surface theory for surface–bulk interactions and its application to mechanics of nanobeams. International Journal of Engineering Science 172, 103624.

Kaplunov, J., Prikazchikov, D.A., 2017. Asymptotic theory for Rayleigh and Rayleigh-type waves. Advances in Applied Mechanics 50, 1–106.

Kaplunov, J., Prikazchikov, D.A., Prikazchikova, L., 2022. On non-locally elastic Rayleigh wave. Philosophical Transactions of the Royal Society A 380, 20210387.

Li, L., Lin, R., Ng, T.Y., 2020. Contribution of nonlocality to surface elasticity. International Journal of Engineering Science 152, 103311.

Mikhasev, G., Erbaş, B., Eremeyev, V.A., 2023. Anti-plane shear waves in an elastic strip rigidly attached to an elastic half-space. International Journal of Engineering Science 184, 103809.

Mikhasev, G., Erbaş, B., Jia, F., 2024. Anti-plane waves in an elastic two-Layer plate with surface effects, in: Yue, X., Yuan, K. (Eds.), Proceedings of 2023 the 6th International Conference on Mechanical Engineering and Applied Composite Materials. MEACM 2023. Mechanisms and Machine Science. Springer, Singapore. volume 156.

Mikhasev, G.I., Botogova, M.G., Eremeyev, V.A., 2021. On the influence of a surface roughness on propagation of anti-plane short-length localized waves in a medium with surface coating. International Journal of Engineering Science 158, 103428.

Mikhasev, G.I., Botogova, M.G., Eremeyev, V.A., 2022. Anti-plane waves in an elastic thin strip with surface energy. Philosophical Transactions of the Royal Society A 380, 20210373–15.

Mindlin, R.D., 1965. Second gradient of strain and surface-tension in linear elasticity. International Journal of Solids and Structures 1, 417–438.

Mishuris, G., Öchsner, A., Kuhn, G., 2006a. FEM-analysis of nonclassical transmission conditions between elastic structures. Part 2: Stiff imperfect interface. CMC: Computers, Materials, & Continua, 4, 137–152.

Mishuris, G.S., Movchan, A.B., Bigoni, D., 2012. Dynamics of a fault steadily propagating within a structural interface. Multiscale Modeling & Simulation 10, 936–953.

Mishuris, G.S., Movchan, A.B., Slepyan, L.I., 2020a. Localized waves at a line of dynamic inhomogeneities: General considerations and some specific problems. Journal of the Mechanics and Physics of Solids 138, 103901.

Mishuris, G.S., Movchan, A.B., Slepyan, L.I., 2020b. Waves in elastic bodies with discrete and continuous dynamic microstructure. Philosophical Transactions of the Royal Society A 378, 20190313.

Mishuris, G.S., Movchan, N.V., Movchan, A.B., 2006b. Steady-state motion of a Mode-III crack on imperfect interfaces. The Quarterly Journal of Mechanics & Applied Mathematics 59, 487–516.

Mogilevskaya, S.G., Zemlyanova, A.Y., Kushch, V.I., 2021. Fiber-and particle-reinforced composite materials with the Gurtin–Murdoch and Steigmann–Ogden surface energy endowed interfaces. Applied Mechanics Reviews 73, 1–18.

Mondal, S., Dhua, S., Nath, A., 2024. Impact of surface/interface elasticity on the propagation of torsional vibration in piezoelectric fiber-reinforced composite and anisotropic medium. Mechanics of Advanced Materials and Structures , 1–21.

Murdoch, A.I., 1976. The propagation of surface waves in bodies with material boundaries. Journal of the Mechanics and Physics of Solids 24, 137–146.

Murdoch, A.I., 1977. The effect of interfacial stress on the propagation of stoneley waves. Journal of Sound and Vibration 50, 1–11.

Murdoch, A.I., 2005. Some fundamental aspects of surface modelling. Journal of Elasticity 80, 33–52.

Newmark, N.M., 1951. Test and analysis of composite beam with incomplete interaction. Proceedings of the Society for Experimental Stress Analysis 9, 75–92.

Rodriguez, C., 2024. Elastic solids with strain-gradient elastic boundary surfaces. Journal of Elasticity , 1–29.

Sharma, B.L., Eremeyev, V.A., 2019. Wave transmission across surface interfaces in lattice structures. International Journal of Engineering Science 145, 103173.

Steigmann, D.J., Ogden, R.W., 1997. Plane deformations of elastic solids with intrinsic boundary elasticity. Proc. Roy. Soc. A: Mathematical, Physical and Engineering Sciences 453, 853–877.

Steigmann, D.J., Ogden, R.W., 1999. Elastic surface-substrate interactions. Proc. Roy. Soc. A: Mathematical, Physical and Engineering Sciences 455, 437–474.

Steigmann, D.J., Ogden, R.W., 2007. Surface waves supported by thin-film/substrate interactions. IMA J. Appl. Math. 72, 730–747.

Überall, H., 1973. Surface waves in acoustics, in: Mason, W.P., Thurston, R.N. (Eds.), Physical Acoustics. Academic Press, New York. volume X.

Wang, J., Huang, Z., Duan, H., Yu, S., Feng, X., Wang, G., Zhang, W., Wang, T., 2011. Surface stress effect in mechanics of nanostructured materials. Acta Mech. Solida Sin. 24, 52–82.

Whitham, G.B., 1999. Linear and Nonlinear Waves. John Wiley & Sons, New Yourk.

Wu, W., Zhang, H., Jia, F., Yang, X., Liu, H., Yuan, W., Feng, X.Q., Gu, B., 2020. Surface effects on frequency dispersion characteristics of Lamb waves in a nanoplate. Thin Solid Films 697, 137831.

Xu, L., Fan, H., 2016. Torsional waves in nanowires with surface elasticity effect. Acta Mechanica 227, 1783–1790.

Xu, L. Wang, X., Fan, H., 2015. Anti-plane waves near an interface between two piezoelectric half-spaces. Mechanics Research Communications 67, 8–12.

Yang, W., Wang, S., Kang, W., Yu, T., Li, Y., 2023. A unified high-order model for size-dependent vibration of nanobeam based on nonlocal strain/stress gradient elasticity with surface effect. International Journal of Engineering Science 182, 103785.

Zhu, F., Pan, E., Qian, Z., Wang, Y., 2019. Dispersion curves, mode shapes, stresses and energies of SH and Lamb waves in layered elastic nanoplates with surface/interface effect. International Journal of Engineering Science 142, 170–184.